Hindawi
Scanning
Volume 2018, Article ID 5736742, 13 pages
https://doi.org/10.1155/2018/5736742

Research Article

Structural and Kinetic Hydrogen Sorption Properties of $Zr_{0.8}Ti_{0.2}Co$ Alloy Prepared by Ball Milling

Hui He,[1] Huaqin Kou,[2,3] Wenhua Luo,[1] Tao Tang,[2] Zhiyong Huang,[2] Ge Sang,[2] Guanghui Zhang,[2] Jingwen Ba,[2] and Meng Liu[2]

[1]*Science and Technology on Surface Physics and Chemistry Laboratory, P.O. Box 9072-35, Mianyang 621908, China*
[2]*Institute of Materials, China Academy of Engineering Physics, P.O. Box 9071-12, Mianyang 621907, China*
[3]*State Key Laboratory of Silicon Materials, Zhejiang University, Hangzhou 310027, China*

Correspondence should be addressed to Huaqin Kou; kouhuaqin@126.com and Wenhua Luo; luowenhua@caep.cn

Received 27 October 2017; Revised 31 December 2017; Accepted 14 January 2018; Published 12 March 2018

Academic Editor: Huaijun Lin

The effects of ball milling on the hydrogen sorption kinetics and microstructure of $Zr_{0.8}Ti_{0.2}Co$ have been systematically studied. Kinetic measurements show that the hydrogenation rate and amount of $Zr_{0.8}Ti_{0.2}Co$ decrease with increasing the ball milling time. However, the dehydrogenation rate accelerates as the ball milling time increases. Meanwhile, the disproportionation of $Zr_{0.8}Ti_{0.2}Co$ speeds up after ball milling and the disproportionation kinetics is clearly inclined to be linear with time at 500°C. It is found from X-ray powder diffraction (XRD) results that the lattice parameter of $Zr_{0.8}Ti_{0.2}Co$ gradually decreases from 3.164 Å to 3.153 Å when the ball milling time extends from 0 h to 8 h, which is mainly responsible for the hydrogen absorption/desorption behaviors. In addition, scanning electron microscope (SEM) images demonstrate that the morphology of $Zr_{0.8}Ti_{0.2}Co$ has obviously changed after ball milling, which is closely related to the hydrogen absorption kinetics. Besides, high-resolution transmission electron microscopy (HRTEM) images show that a large number of disordered microstructures including amorphous regions and defects exist after ball milling, which also play an important role in hydrogen sorption performances. This work will provide some insights into the principles of how to further improve the hydrogen sorption kinetics and disproportionation property of $Zr_{0.8}Ti_{0.2}Co$.

1. Introduction

Because of the rapid decrease of fossil fuels and the increasingly serious environmental pollution in recent years, developing a clean and renewable energy has become an urgent task for mankind [1]. Under the development of ITER (International Thermonuclear Experimental Reactor), fusion energy, by burning the fuel of deuterium (D) and tritium (T) plasma, is regarded as one of the most ideal energy sources due to its huge energy release, abundant fuel resources, and low radioactivity [2–4]. In order to ensure the successful operation of fusion reactors, a viable, highly efficient, safe, and inexpensive hydrogen isotope storage method for D-T fuel is very necessary [5, 6].

In ITER, the D-T fuel is recommended to be stored as metal deuteride and tritide because solid-state hydrogen isotopes storage offers such advantages as safety, efficiency (higher bulk hydrogen storage density), and processing convenience over gas and liquid storage methods [7, 8]. Among several alternative hydrogen storage materials, an intermetallic compound of ZrCo is proposed as one of the most suitable candidates for tritium storage according to (1), since it possesses such excellent properties as low equilibrium hydrogen pressure and fast hydrogen absorption rate at room temperature, moderate temperature for hydrogen desorption to 100 kPa, and desirable features of safety like nonradioactivation, low pyrophoricity, and small volume expansion during hydrogen sorption cycles [9–14].

$$2ZrCoH_3 \longleftrightarrow 2ZrCo + 3H_2 \quad (1)$$

However, its serious degradation of hydrogen storage properties during the hydrogen sorption cycle obstructs its

wide application, resulting from the concomitant hydrogen-induced disproportionation reaction that happened above 573 K during hydrogen sorption process shown as follows[15–18]:

$$2ZrCo + H_2 \longrightarrow ZrH_2 + ZrCo_2 \quad (2a)$$

$$2ZrCoH_3 \longrightarrow ZrH_2 + ZrCo_2 + 2H_2 \quad (2b)$$

Because of the high thermodynamic stabilities of ZrH_2 and $ZrCo_2$, the disproportionation of ZrCo will cause significant degradation of hydrogen storage properties during the practical hydrogen sorption cycles [19].

Recently, many investigations mainly focused on element substitution have been made to improve the antidisproportionation property of ZrCo, which achieved remarkable progress [20–24]. Compared with other elements, Ti has been surprisingly found to be the most effective substitution element for improving the antidisproportionation property so far. Huang et al. [25] found that the equilibrium hydrogen desorption pressure of $Zr_{1-x}Ti_xCo$ alloy increases along with increasing Ti content. In the meantime, hydrogen sorption cycles do not produce separated ZrCo, TiCo, and ZrH_2, suggesting that the antidisproportionation property of ZrCo alloy is improved by Ti substitution. Zhao et al. also confirmed that partial substitution of Ti for Zr will significantly enhance the antidisproportionation property of ZrCo [26, 27]. Zhang et al. [28] systematically compared the effects of Ti substitution on the disproportionation behaviors of ZrCo with Sc, Ni, and Fe elements. It was observed that Ti has superior effect on suppressing the disproportionation of ZrCo. Similar result was proved by Kou et al. who reported that $Zr_{0.8}Ti_{0.2}Co$ bed had better durability against disproportionation than ZrCo bed and $Zr_{0.8}Hf_{0.2}Co$ bed [29]. Meanwhile, Jat et al. [30] further investigated the influences of Ti amount on the disproportionation rate of $Zr_{1-x}Ti_xCo$ alloy and found the disproportionation decreases in order of $ZrCo > Zr_{0.9}Ti_{0.1}Co > Zr_{0.7}Ti_{0.3}Co > Zr_{0.8}Ti_{0.2}Co$.

Although it seems that Ti-substituted ZrCo alloy possesses the improved antidisproportionation property, the requirements of practical application still cannot be completely satisfied due to its stagnant hydrogen sorption kinetics. Zhao et al. [26] reported that the hydrogen absorption amount and rate of ZrCo decrease with the Ti content increasing. Moreover, Shmayda et al. [31] and Yoo et al. [32] showed that the kinetic response of ZrCo for hydrogen sorption is slower than uranium, which restricts the application of ZrCo alloy. Therefore, it is of great necessity to further enhance the hydrogen sorption kinetics of Ti-substituted ZrCo alloy.

It has extensively shown that mechanical ball milling is an effective technique for improving the kinetic property of hydrogen storage materials [33–36]. However, the effects of ball milling on the hydrogen sorption kinetics and microstructure of ZrCo-based alloy have never been investigated. In this paper, we focused on the effects of ball milling on microstructure and kinetic hydrogen sorption properties of $Zr_{0.8}Ti_{0.2}Co$ alloy. Furthermore, because study of kinetics is clearly beneficial to understanding of mechanism about hydrogen sorption process [20, 37, 38], kinetic analysis has also been carried out for disproportionation of $Zr_{0.8}Ti_{0.2}Co$ in this work.

2. Experimental

2.1. Sample Preparation and Kinetic Measurements. $Zr_{0.8}Ti_{0.2}Co$ powder with particle size of 2~4 mm was purchased from the General Research Institute for Nonferrous Metals (Beijing, China). The hydrogen sorption behaviors of the samples were investigated by a Sievert type apparatus. The detailed activation procedures of $Zr_{0.8}Ti_{0.2}Co$ were performed according to [39]. The samples were prepared by ball milling of $Zr_{0.8}Ti_{0.2}Co$ powder using a planetary mill at 400 rpm for different time. After ball milling, the samples were firstly evacuated at 500°C, and then the hydrogen absorption measurements of samples were conducted at 100°C under 0.8 bar H_2. For each time, about 1 g sample was loaded in the reactor of the apparatus, and hydrogen pressure reduction of ~0.2 bar was achieved for hydrogenation. After hydrogenation, the hydrogen in the reactor was evacuated and then the dehydrogenation measurements of samples were carried out from room temperature to 500°C with heating rate of 5°C/min. After that, the isothermal disproportionation kinetics was examined at 500°C for more than 500 min. The change of hydrogen pressure (P) as a function of time was recorded from room temperature to the end of the isothermal period. During the whole dehydrogenation process, the initial hydrogen pressure was recorded as P_0 and the maximum addition of hydrogen pressure was denoted as P_{max}. As a result, the hydrogen desorption and disproportionation of the sample were quantified by formula as $(P - P_0)/P_{max}$.

2.2. Structural Characterizations. X-ray powder diffraction (XRD) method was used to characterize the crystal structures of $Zr_{0.8}Ti_{0.2}Co$ samples at different states on a DX2700B diffractometer with Cu K_a radiation, 40 kV, and 30 mA. The XRD patterns were recorded in steps of 0.02° (2θ) from 20° to 90° with a constant scanning rate of 0.6 s per step. For Rietveld refinement of lattice parameters, special XRD data was obtained by scanning rate of 1.8 s per step.

The morphology of the samples was studied by scanning electron microscope (SEM, Ultra55, CARL ZEISSNTS GmbH) and the compositional analysis on surface was carried out using energy dispersive X-ray spectroscopy (EDS, Inca). Morphological observation inside the particle was carried out by Helios Nanolab 600i Focused Ion Beam (FIB) using beam energy of 20 keV and a beam current of 2.8 nA. The microstructure of the samples was investigated using high-resolution transmission electron microscopy (HRTEM, Libra 200, CARL ZEISS IRTS) with an accelerating voltage of 200 kV.

3. Results and Discussion

3.1. Hydrogen Absorption/Desorption Kinetics. Figure 1 represents the XRD patterns of activated $Zr_{0.8}Ti_{0.2}Co$ samples after ball milling for different time. It can be found that $Zr_{0.8}Ti_{0.2}Co$ samples still keep ZrCo phase except for trace

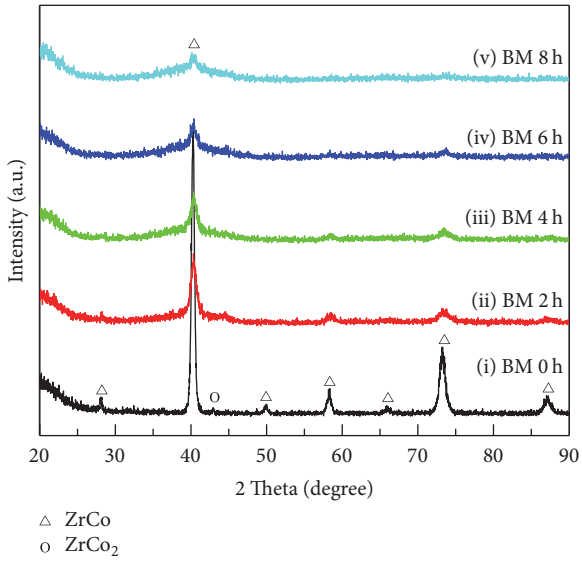

FIGURE 1: XRD patterns of the activated $Zr_{0.8}Ti_{0.2}Co$ samples after ball milling for different time. (i) 0 h; (ii) 2 h; (iii) 4 h; (iv) 6 h; (v) 8 h.

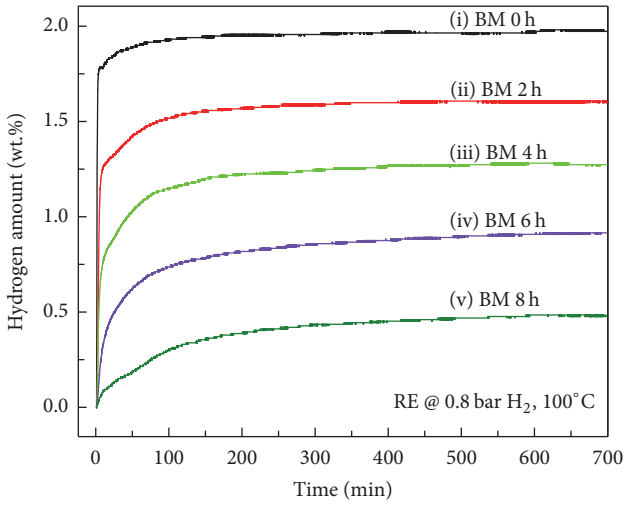

FIGURE 2: Hydrogen absorption curves of $Zr_{0.8}Ti_{0.2}Co$ samples under 0.8 bar H_2 at 100°C after ball milling for different time. (i) 0 h; (ii) 2 h; (iii) 4 h; (iv) 6 h; (v) 8 h.

amount of $ZrCo_2$ phase, which is identical with previous researches [26, 27]. Meanwhile, it is clear that the intensities of ZrCo diffraction peaks decrease and the peaks exhibit broadened characteristics with increasing ball milling time. It is suggested that the crystalline structure of ZrCo phase may be damaged and the average grain size of samples should decrease during the ball milling process [40].

The hydrogen absorption curves of $Zr_{0.8}Ti_{0.2}Co$ samples after ball milling for different time are displayed in Figure 2. Since the disproportionation reactions of ZrCo alloy shown as (2a) and (2b) usually take place at high temperature, the curves in Figure 2 should represent the hydrogenation reaction shown as (1). Obviously, the hydrogen absorption amount decreases with increasing ball milling time. The hydrogenation amount reaches 1.97 wt.% for the sample without ball milling, whereas the total hydrogen amount of only 0.50 wt.% can be obtained for the sample ball milled for 8 h. Meanwhile, the hydrogen absorption rate also exhibits a tendency to slow down after ball milling.

The dehydrogenation curves of ball milled $Zr_{0.8}Ti_{0.2}Co$ samples after hydrogenation are shown in Figure 3. According to (2a) and (2b), the disproportionation reaction displayed by (2b) only happens under high hydrogen pressure. However, the hydrogen pressure is lower than 1 bar in this study. Therefore, the disproportionation of $Zr_{0.8}Ti_{0.2}Co$ sample only takes place according (2a) in this work, which causes the reduction in hydrogen pressure. As a result, the whole hydrogen desorption curve in Figure 3 can be divided into two stages, respectively, belonging to the temperature programmed dehydrogenation process (Figure 3(b)) and the disproportionation process (Figure 3(c)). It can be observed from the first stage that the hydrogen desorption rate is enhanced with increasing ball milling time, which is beneficial to practical application of ZrCo-based alloy. The second stage substantially represents an isothermal disproportionation process at 500°C. It can be seen that the disproportionation extent is very slight and the disproportionation rate is slow for all samples at 500°C, which is very close to the result reported by Zhang et al. [28]. Nevertheless, it is readily discernible that the disproportionation rate and extent monotonously grow with increasing ball milling time. These results suggest that not only the dehydrogenation rate but also the disproportionation rate of $Zr_{0.8}Ti_{0.2}Co$ can be quickened by ball milling, the mechanism of which will be specifically discussed below.

Figure 4 demonstrates XRD patterns of the ball milled $Zr_{0.8}Ti_{0.2}Co$ samples after disproportionation shown in Figure 3. It can be seen that the diffraction peaks corresponding to ZrCo phase are clearly present in all samples, though the intensity of ZrCo peaks decreases slightly with increasing ball milling time. The existence of major phase of ZrCo illustrates that the dehydrogenation mainly proceeds according to (1). In addition, the weak diffraction peaks of disproportionation products including ZrH_2 and $ZrCo_2$ can be carefully observed, indicating the disproportionation extent of $Zr_{0.8}Ti_{0.2}Co$ sample should be small. The intensity of diffraction peaks for ZrH_2 and $ZrCo_2$ is well in agreement with the disproportionation behaviors displayed in Figure 3, which shows minor reduction in hydrogen pressure.

3.2. Structural Characterization and Kinetic Mechanism. From the results above, it can be found that the hydrogen desorption kinetics and disproportionation kinetics of $Zr_{0.8}Ti_{0.2}Co$ become faster, while the hydrogenation kinetics is restrained by ball milling. To comprehend these kinetic behaviors, detailed structural characterizations were performed. Firstly, the phase structure variation after ball milling has been investigated. To determine the lattice parameters of $Zr_{0.8}Ti_{0.2}Co$ samples as accurately as possible, special XRD experiments have been performed to obtain strong diffraction signal by increasing the scanning time. According to the XRD results, the lattice parameters of the samples have been calculated by Rietveld refinement of XRD data via Jade

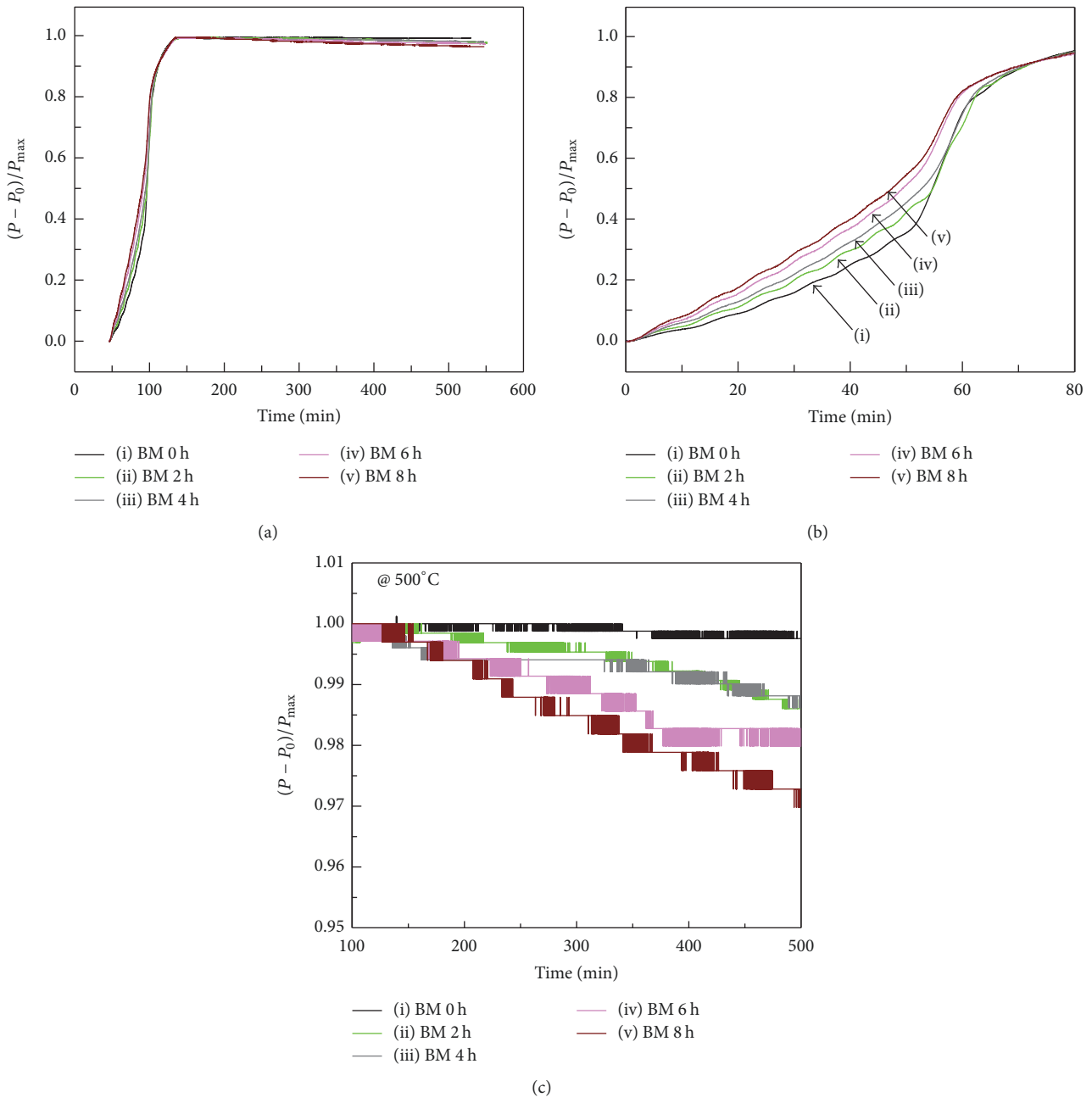

FIGURE 3: Dehydrogenation curves (a), enlarged dehydrogenation curves (b), and enlarged disproportionation curves (c) of $Zr_{0.8}Ti_{0.2}Co$ samples ball milled for different time. (i) 0 h; (ii) 2 h; (iii) 4 h; (iv) 6 h; (v) 8 h.

6.0 software. The representative Rietveld refinement pattern of $Zr_{0.8}Ti_{0.2}Co$ sample is shown in Figure 5. The refinement result shows that the crystal structure of $Zr_{0.8}Ti_{0.2}Co$ sample without ball milling is CsCl-type cubic (bcc) with lattice parameter $a = 3.1638$ Å, which is in good agreement with other study [28]. According to the specific Rietveld refinement results as displayed in Table 1, the lattice parameter and cell volume of $Zr_{0.8}Ti_{0.2}Co$ sample slightly and continuously decrease with increasing ball milling time, which may be probably attributed to cumulative plastic deformation and microstrain in the crystal lattice during the ball milling process [33, 40]. In view of the variation of lattice parameter, it is easy to understand the kinetic performances of $Zr_{0.8}Ti_{0.2}Co$ after ball milling. When the lattice parameter and cell volume become smaller, the occupancy of H atom in interstitial sites will become more difficult but release of H atom from interstitial sites will be easier [41]. Hence, it is observed that hydrogen absorption kinetics decreases but hydrogen desorption kinetics increases for $Zr_{0.8}Ti_{0.2}Co$ with increasing ball milling time.

To investigate the morphologies of ball milled $Zr_{0.8}Ti_{0.2}Co$ samples, SEM analysis has been performed and

Table 1: Rietveld refinement results of XRD patterns of $Zr_{0.8}Ti_{0.2}Co$ samples after ball milling for different time.

System	Ball milling time/hour	Space group	Lattice parameters of major constituent phase (ZrCo phase)/Å	Cell volume of major constituent phase (ZrCo phase)/Å^3
ZrCo [13]	0	*Pm-3m*	3.1957	32.64
$Zr_{0.8}Ti_{0.2}Co$	0	*Pm-3m*	3.1638	31.67
	2		3.1587	31.55
	4		3.1574	31.48
	6		3.1555	31.42
	8		3.1534	31.35

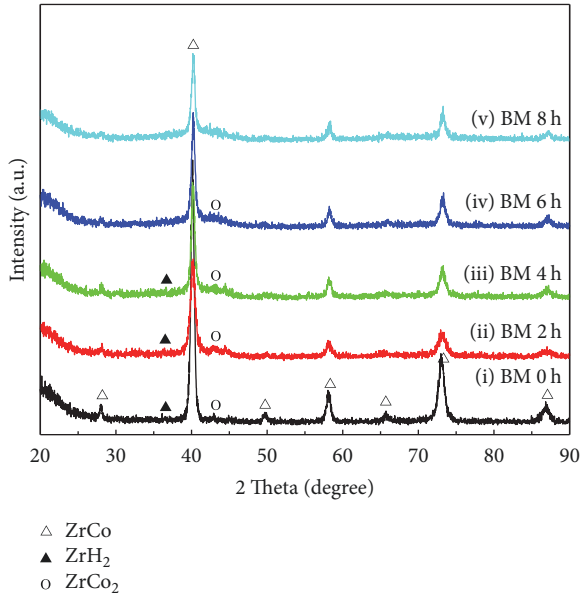

Figure 4: XRD patterns of the ball milled $Zr_{0.8}Ti_{0.2}Co$ samples after disproportionation. (i) 0 h; (ii) 2 h; (iii) 4 h; (iv) 6 h; (v) 8 h.

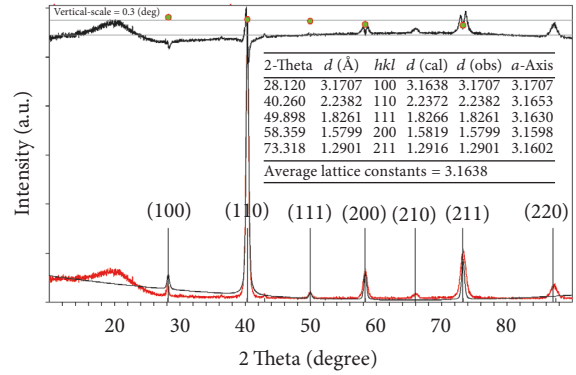

Figure 5: Rietveld refinement of X-ray diffraction pattern of $Zr_{0.8}Ti_{0.2}Co$ sample without ball milling.

the results are shown in Figure 6. After ball milling, the morphologies of $Zr_{0.8}Ti_{0.2}Co$ sample tend to be small particles from initial chip. Meanwhile, the particle size gradually decreases with increasing the ball milling time. Besides, as the ball milling time increases, the agglomeration of particles is distinctly reduced and the particles become more dispersive.

Furthermore, in order to closely observe the surface of the samples, the SEM images of the ball milled $Zr_{0.8}Ti_{0.2}Co$ samples at magnification of 10000x were obtained, as shown in Figure 7. A lot of chips and sharp edges are observed for the sample without ball milling. However, the sharp edges can hardly be observed on the surface of ball milled $Zr_{0.8}Ti_{0.2}Co$ sample, which should be caused by deformation and compaction during the ball milling process. It is well known that the edges are apt to break off and fresh surface will emerge in the process of hydrogenation [42, 43], which is beneficial to enhancement of hydrogen absorption. Moreover, as a direct and fast diffusion path of hydrogen, the edges are also beneficial to fast hydrogen absorption [44]. Hence, the change in morphology is mainly responsible for the decrease of hydrogen absorption kinetics for $Zr_{0.8}Ti_{0.2}Co$ samples after ball milling.

In order to analyze the composition of the sample surface, two representative EDS spectrums of every sample over the surface were obtained, as shown in Figure 8. The detailed elemental contents for every sample are listed in Table 2. It is interesting to discover that the existence of Fe element on the surface of particles is detected for all ball milled $Zr_{0.8}Ti_{0.2}Co$ samples. This suggests that the Fe element may be brought by steel milling vessel and balls during the ball milling process [38]. It has been reported that the disproportionation of ZrCo will be accelerated after doping Fe [22, 28]. Hence, it is reasonable to believe that faster disproportionation rate of ball milled $Zr_{0.8}Ti_{0.2}Co$ samples has direct correlation with the introduced Fe element on the surface of particles. Besides, it can be found that the average atom ratio of (Zr + Ti)/(Co + Fe) for the selected regions decreases gradually from 0.89 to 0.66 when the ball milling time extends from 0 h to 8 h. As previous studies proved, when the average atom ratio of Zr : Co is much closer to 0.5 (1 : 2), the elemental recombination of $ZrCo_2$ phase will be facilitated during the disproportionation process [45, 46]. Consequently, disproportionation of ZrCo is aggravated. Due to the analogical feature of group element, the substitution element of Ti and introduced Fe can, respectively, be included in Zr and Co. As a result, the gradual decrease of (Zr + Ti)/(Co + Fe) from 0.89 to 0.66 may be another reason that aggravates the disproportionation of $Zr_{0.8}Ti_{0.2}Co$ sample by increasing ball milling time, as shown in Figure 3.

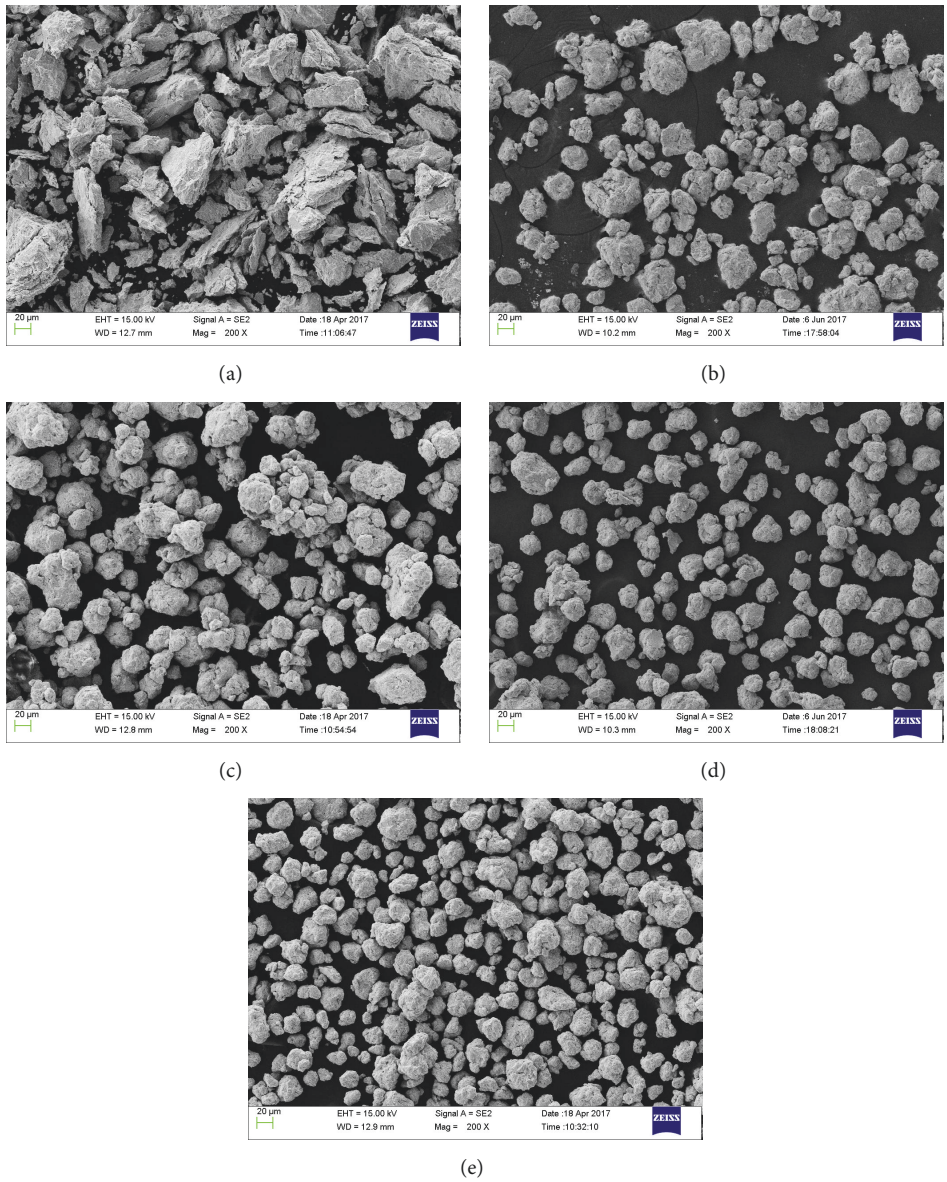

Figure 6: SEM images of the $Zr_{0.8}Ti_{0.2}Co$ samples ball milled for different time. (a) 0 h; (b) 2 h; (c) 4 h; (d) 6 h; (e) 8 h.

In order to further characterize the microstructure, the TEM analysis for $Zr_{0.8}Ti_{0.2}Co$ samples ball milled for 8 h has been employed and the results are shown in Figure 9. Figures 9(b) and 9(c), respectively, show enlarged TEM images and corresponding SAED patterns of zones 1 and 2 in Figure 9(a). It can be found from the SAED patterns that the $Zr_{0.8}Ti_{0.2}Co$ particle ball milled for 8 h is comprised of not only polycrystalline regions but also a number of amorphous regions. In accordance with PDF number 030657272, the interplanar distances of 0.218 nm, 0.218 nm, and 0.219 nm in Figure 9(b) all correspond to {110} planes of $Zr_{0.8}Ti_{0.2}Co$. According to Figure 5, the interplanar distance of {110} should be 0.224 nm for $Zr_{0.8}Ti_{0.2}Co$ sample without ball milling. It is clear that the interplanar distance of {110} has been shortened to be about 0.218 nm after ball milling for 8 h. It is suggested that the lattice parameter of $Zr_{0.8}Ti_{0.2}Co$ sample was decreased after ball milling, which is in good agreement with the Rietveld refinement results of XRD. Moreover, a number of amorphous regions (over yellow line) are clearly observed in Figure 9(c). Meanwhile, a large number of defects including dislocations and grain boundaries (around green line) are widely observed, which provide a possible explanation for the broadened XRD patterns shown in Figure 1. As well known, these disordered microstructures mentioned above are favorable for H atom diffusion instead of occupation [38, 47]. Therefore, the reduction of the hydrogenation amount and enhancement of the dehydrogenation rate for ball milled $Zr_{0.8}Ti_{0.2}Co$ samples are probably resulting from the disordered microstructures produced during the ball milling process.

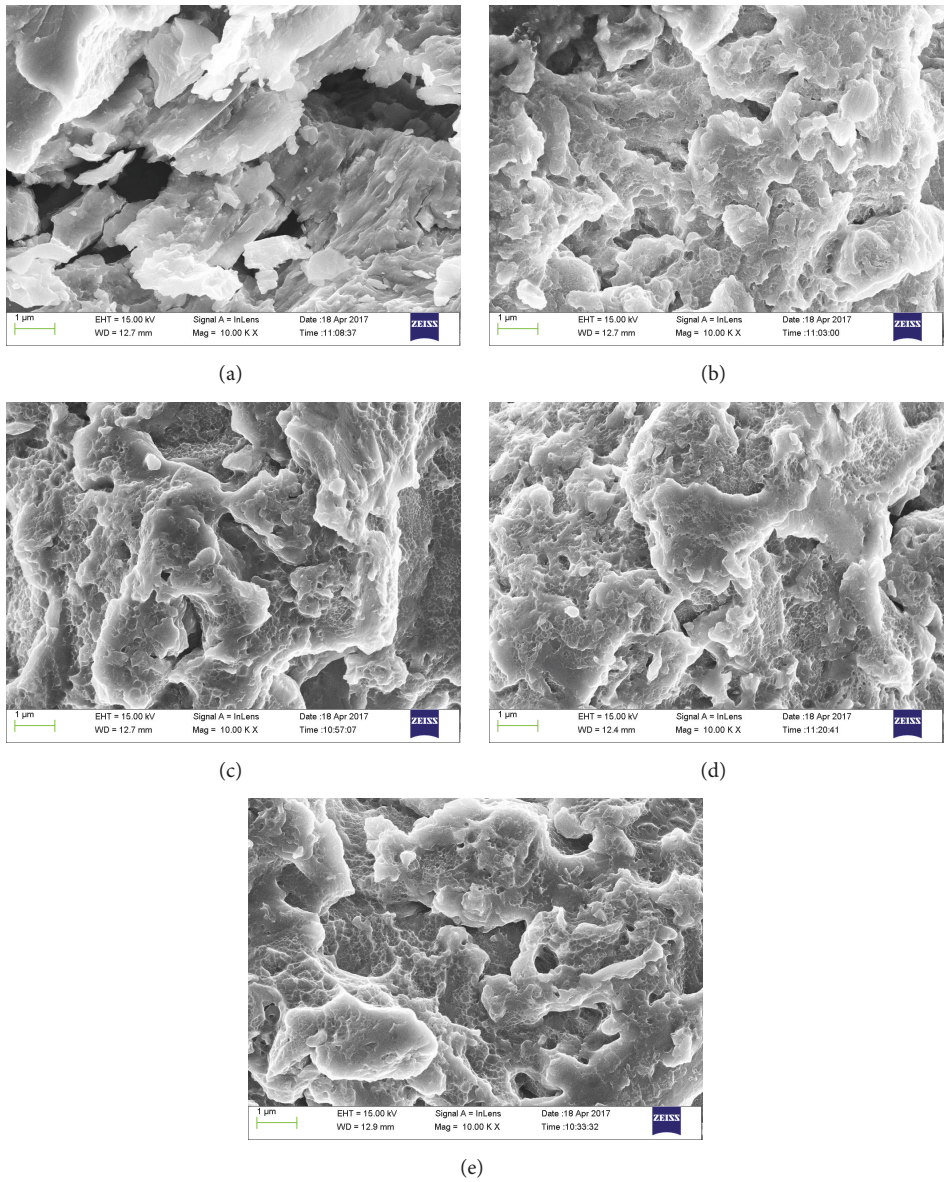

FIGURE 7: SEM images of the $Zr_{0.8}Ti_{0.2}Co$ samples after ball milling for different time at magnification of 10000x. (a) 0 h; (b) 2 h; (c) 4 h; (d) 6 h; (e) 8 h.

3.3. Kinetic Model Analysis. In order to further understand the disproportionation kinetic mechanism, the kinetic analysis of disproportionation has been performed for ball milled $Zr_{0.8}Ti_{0.2}Co$. Usually, the relationship between the reacted fraction and reaction time is linear for surface reaction controlled step [48, 49]. According to Figure 3, it can been found that the disproportionation curves of all $Zr_{0.8}Ti_{0.2}Co$ samples should just represent the initial stage of whole disproportionation and the reaction equilibrium has not been reached within 450 min at 500°C. Moreover, the disproportionation kinetics of all $Zr_{0.8}Ti_{0.2}Co$ samples in this stage is clearly inclined to be linear. Thus, the isothermal disproportionation data of $Zr_{0.8}Ti_{0.2}Co$ sample after ball milling for different time has been linearly fitted, as shown in Figure 10. It can be seen from the fitting results that the disproportionation kinetics of $Zr_{0.8}Ti_{0.2}Co$ samples is much closer to linear with increasing the ball milling time. Meanwhile, the slope of fitted line is slightly decreased, corresponding to the slight aggravation of disproportionation rate. The well-fitted linear results suggest that the disproportionation stage of $Zr_{0.8}Ti_{0.2}Co$ samples curved by Figure 3 should be a surface reaction controlled step.

Based on the results of microstructure and kinetic analysis above, some useful insights can be obtained into the mechanism of hydrogen sorption reaction and disproportionation reaction for ball milled $Zr_{0.8}Ti_{0.2}Co$ samples. The effects of ball milling on the hydrogen sorption and disproportionation behaviors of $Zr_{0.8}Ti_{0.2}Co$ sample can be deduced from the changed microstructure including lattice parameter, morphology, elemental composition, and crystal defects. For

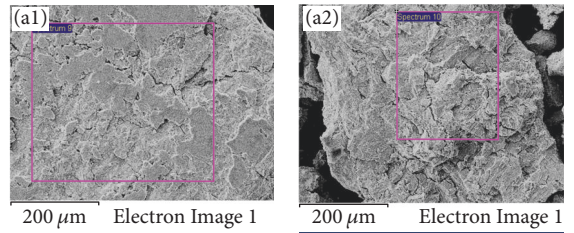

Element	Weight%	Atomic%
Ti K	1.23	9.73
Co K	8.08	52.01
Zr L	9.20	38.26
Total	18.51	

Element	Weight%	Atomic%
Ti K	1.04	10.43
Co K	6.67	54.28
Zr L	6.71	35.30
Total	14.42	

(a)

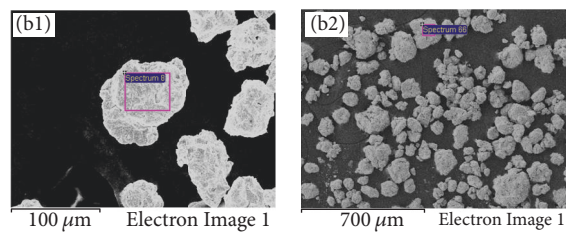

Element	Weight%	Atomic%
Ti K	1.09	8.40
Fe K	1.60	10.58
Co K	7.09	44.56
Zr L	8.98	36.47
Total	18.76	

Element	Weight%	Atomic%
Ti K	0.45	7.77
Fe K	0.79	11.71
Co K	3.30	46.27
Zr L	3.79	34.26
Total	8.33	

(b)

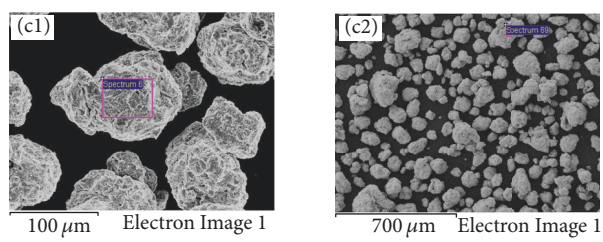

Element	Weight%	Atomic%
Ti K	1.18	9.26
Fe K	1.65	11.11
Co K	6.92	44.30
Zr L	8.55	35.34
Total	18.30	

Element	Weight%	Atomic%
Ti K	0.33	8.06
Fe K	0.55	11.60
Co K	2.40	47.85
Zr L	2.53	32.49
Total	5.81	

(c)

Figure 8: Continued.

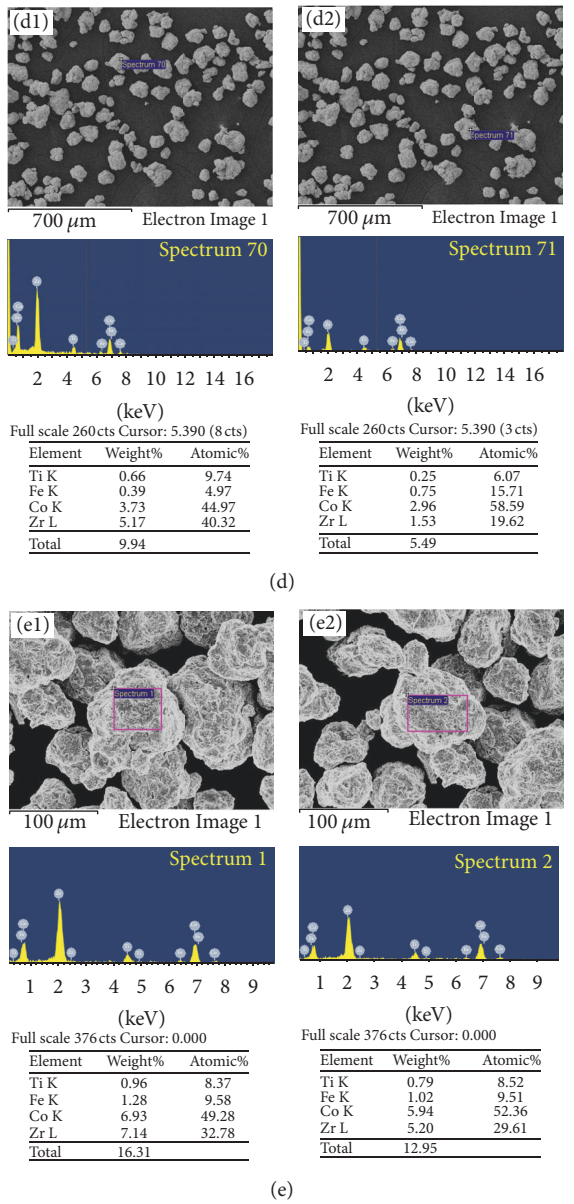

Figure 8: EDS results of the $Zr_{0.8}Ti_{0.2}Co$ samples after ball milling for different time. (a) 0 h; (b) 2 h; (c) 4 h; (d) 6 h; (e) 8 h.

hydrogen sorption reaction, it can be found that ball milling shows negative effect on the hydrogen absorption rate of $Zr_{0.8}Ti_{0.2}Co$ sample, which is different from the commonly positive effects of ball milling on hydrogen storage materials in many studies. The negative effects of ball milling may be resulting from three aspects: (1) the decreased cell volume makes the entering of hydrogen atom into interstitial site in lattice more difficult; (2) the missing sharp edges of particles cut the paths for fast transfer of hydrogen; (3) the increased disorderliness of microstructure goes against the occupation of hydrogen. As a result, it was observed that the hydrogen absorption rate and amount of $Zr_{0.8}Ti_{0.2}Co$ sample were decreased by increasing ball milling. On the other hand, it can be found that the ball milling plays a positive role in hydrogen desorption rate. The positive effects of ball milling may be derived from three points: (1) the decreased cell volume results in the fact that H atoms begin to be less-stable in the crystal lattice and are inclined to leave from crystal interstitial sites; (2) the introduced Fe on the surface may act as catalysts for hydrogen dissociation [50]; (3) the produced lattice defects like dislocations and grain boundaries possibly act as a pathway for hydrogen transportation during dehydrogenation [51, 52]. Consequently, it was seen that the hydrogen desorption rate was increased by ball milling.

For disproportionation reaction, it is found the disproportionation rate of $Zr_{0.8}Ti_{0.2}Co$ sample was exacerbated by ball milling. According to the kinetic analysis, the disproportionation stage of $Zr_{0.8}Ti_{0.2}Co$ in this work should be a surface reaction controlled step, indicating that the surface state is very important for the disproportionation.

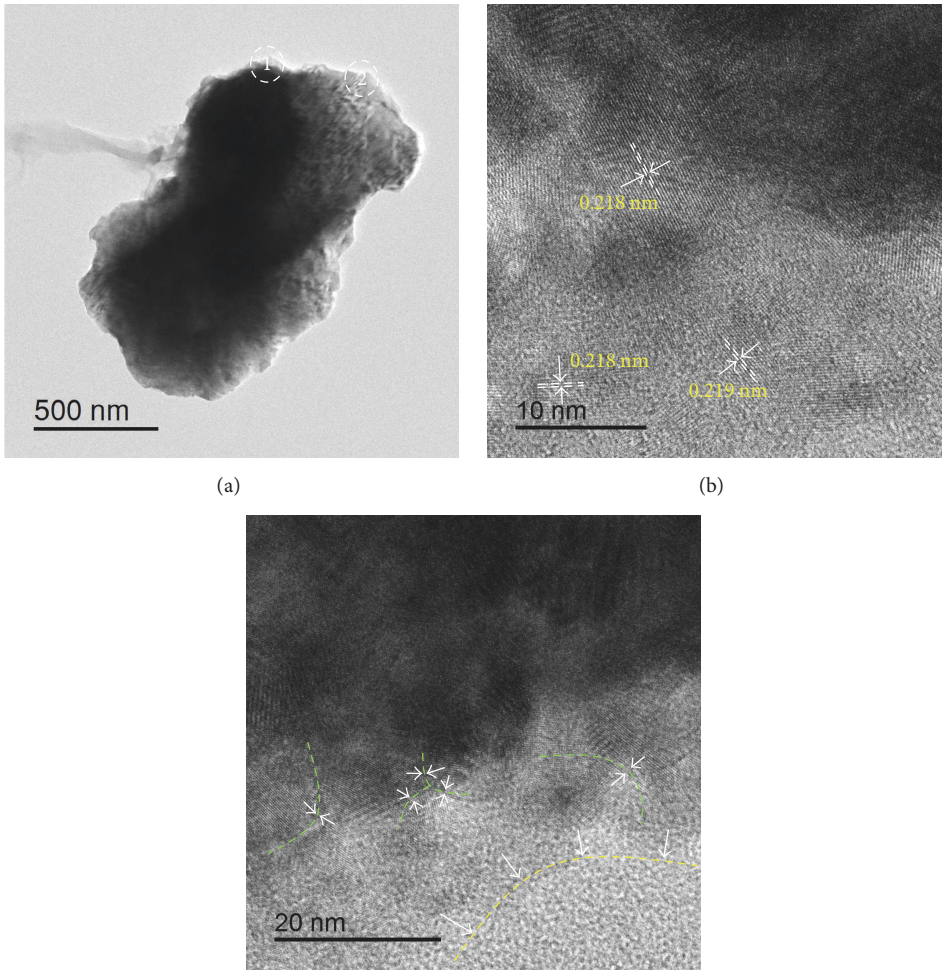

(a) (b)

(c)

Figure 9: TEM analysis of $Zr_{0.8}Ti_{0.2}Co$ sample for ball milled for 8 h. (a) Low-magnification image of particle; (b) high-resolution image of peripheral zone 1 in (a); (c) high-resolution image of peripheral zone 2 in (a).

Table 2: EDS results of elemental composition for selected regions of $Zr_{0.8}Ti_{0.2}Co$ samples after ball milling for different time.

ZrCo samples	Selected region	Zr (atomic%)	Ti (atomic%)	Co (atomic%)	Fe (atomic%)	(Zr + Ti)/(Co + Fe)
BM 0 h	1#	38.26	9.73	52.01		
	2#	38.49	7.48	54.04		
	Average	38.38	8.61	53.03		0.89
BM 2 h	1#	36.47	8.40	44.56	10.58	
	2#	34.26	7.77	46.27	11.71	
	Average	35.37	8.09	45.42	11.15	0.77
BM 4 h	1#	35.34	9.26	44.3	11.11	
	2#	32.49	8.06	47.85	11.60	
	Average	33.92	8.66	46.08	11.36	0.74
BM 6 h	1#	37.43	8.71	45.97	7.90	
	2#	28.83	7.2	56.89	7.08	
	Average	33.13	7.96	51.43	7.49	0.70
BM 8 h	1#	32.78	8.37	49.28	9.58	
	2#	29.61	8.52	52.36	9.51	
	Average	31.20	8.45	50.82	9.55	0.66

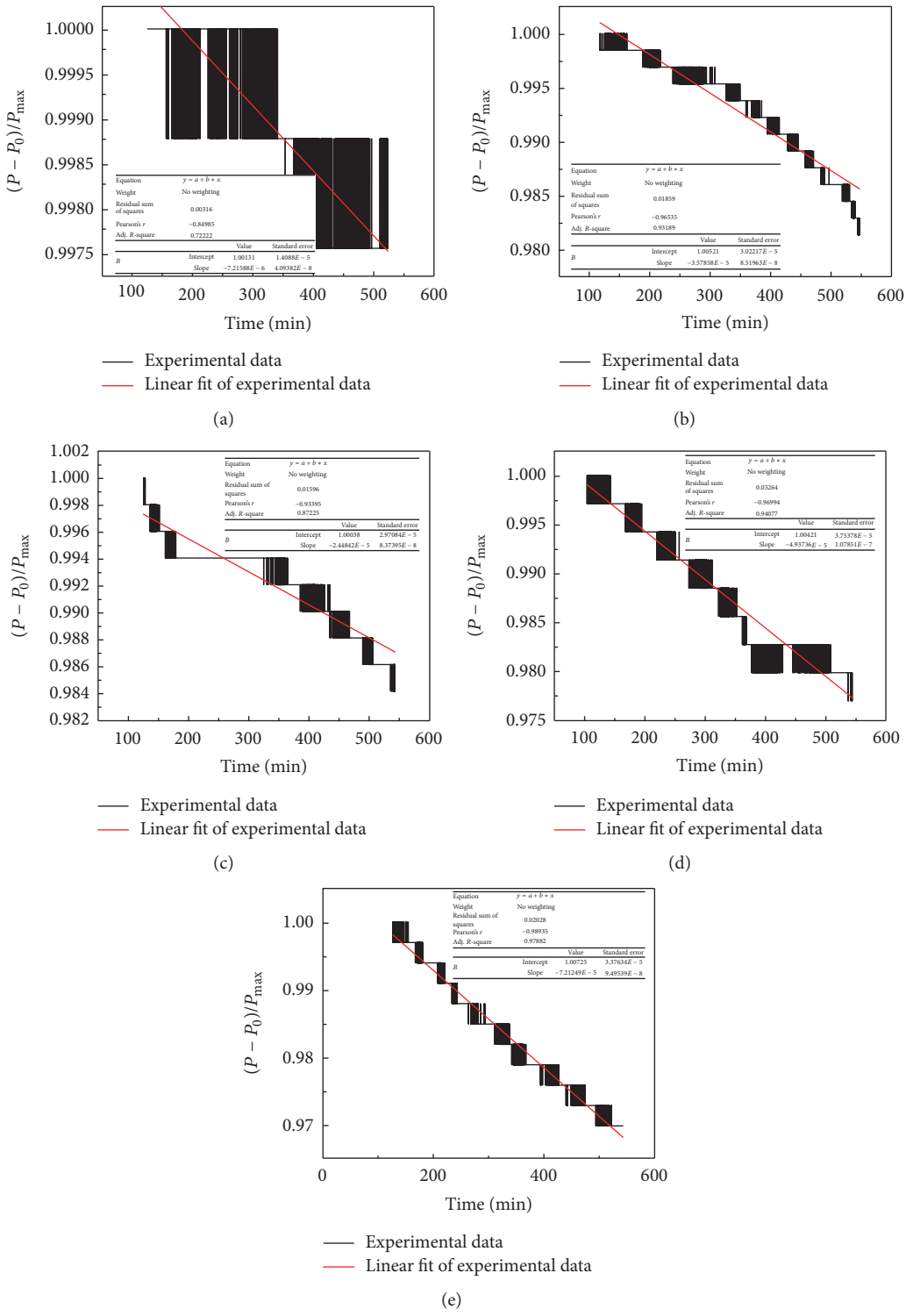

FIGURE 10: The linear fitting results of disproportionation kinetics for $Zr_{0.8}Ti_{0.2}Co$ samples after ball milling for different time. (a) 0 h; (b) 2 h; (c) 4 h; (d) 6 h; (e) 8 h.

As mentioned in the analysis of EDS results, Fe element was introduced during the ball milling process on the surface of $Zr_{0.8}Ti_{0.2}Co$ particles, resulting in the gradual decrease of (Zr + Ti)/(Co + Fe). This possibly facilitates the elemental recombination of $ZrCo_2$ phase. So, it is observed that the ball milled $Zr_{0.8}Ti_{0.2}Co$ owns faster disproportionation kinetics. On the other hand, it is found from the microstructure that considerable crystal defects and strain energy were formed after ball milling, especially on the surface. It is well known that the crystal defects and strain energy will

facilitate the transfer process of hydrogen atoms during hydrogen sorption reaction, which may be also beneficial for promoting the transfer of hydrogen atom from ZrCo to form ZrH_2. Consequently, it is observed that the rate of the initial disproportionation stage for $Zr_{0.8}Ti_{0.2}Co$ is enhanced by ball milling. In conclusion, if $Zr_{0.8}Ti_{0.2}Co$ is expected to not only own fast hydrogen sorption kinetics but also have good antidisproportionation, it may be a good way to prepare $Zr_{0.8}Ti_{0.2}Co$ as fine powder with smaller lattice parameter, uniform element distribution, and orderly microstructure and without impurity.

4. Conclusion

In summary, the effects of ball milling on the hydrogen sorption properties and microstructure of $Zr_{0.8}Ti_{0.2}Co$ have been investigated systematically. Experimental results show that hydrogen absorption kinetics of $Zr_{0.8}Ti_{0.2}Co$ decreases and the hydrogen desorption kinetics accelerates with increasing the ball milling time. Meanwhile, the disproportionation rate of $Zr_{0.8}Ti_{0.2}Co$ is aggravated after ball milling. Characterizations of microstructure reveal that the variation of hydrogen sorption kinetics for $Zr_{0.8}Ti_{0.2}Co$ after ball milling is mainly resulting from the changed microstructure including lattice parameter, morphology, elemental composition, and crystal defects. Kinetic analysis reveals that the initial stage of disproportionation for $Zr_{0.8}Ti_{0.2}Co$ is a surface step controlled reaction. And the slight aggravation of disproportionation rate may be attributed to the introduced Fe on the surface of particles and the crystal defects together with strain energy after ball milling.

Conflicts of Interest

The authors declare that they have no conflicts of interest.

Acknowledgments

This work was financially supported by the Foundation of President of China Academy of Engineering Physics (no. YZJJLX2017008), Development Foundation of China Academy of Engineering Physics for Science and Technology (no. 2015B0302067), National Magnetic Confinement Fusion Science Program of China, Open Project of State Key Laboratory of Silicon Materials (SKL2016-10), and National Natural Science Foundation of China (nos. 21573200, 21601165, and 51731002). The authors would like to thank Mr. Weidong Liu and Ms. Ping Zhao for their assistance in experiments and Dr. Huan Wang for fruitful discussions.

References

[1] H. Lund, "Renewable energy strategies for sustainable development," *Energy*, vol. 32, no. 6, pp. 912–919, 2007.

[2] J. Ongena, R. Koch, R. Wolf, and H. Zohm, "Magnetic-confinement fusion," *Nature Physics*, vol. 12, no. 5, pp. 398–410, 2016.

[3] D. Clery, "Private fusion machines aim to beat massive global effort," *Science*, vol. 356, no. 6336, pp. 360-361, 2017.

[4] W. Wayt Gibbs, "Fusion reactor fuels up with bomb ingredient," *Science*, vol. 354, no. 6313, pp. 690-691, 2016.

[5] N. Holtkamp, "An overview of the ITER project," *Fusion Engineering and Design*, vol. 82, no. 5–14, pp. 427–434, 2007.

[6] M. Glugla, R. Lässer, L. Dörr, D. K. Murdoch, R. Haange, and H. Yoshida, "The inner deuterium/tritium fuel cycle of ITER," *Fusion Engineering and Design*, vol. 69, no. 1-4, pp. 39–43, 2003.

[7] R. Bhattacharyya and S. Mohan, "Solid state storage of hydrogen and its isotopes: an engineering overview," *Renewable & Sustainable Energy Reviews*, vol. 41, pp. 872–883, 2015.

[8] L. Schlapbach and A. Züttel, "Hydrogen-storage materials for mobile applications," *Nature*, vol. 414, no. 6861, pp. 353–358, 2001.

[9] M. Glugla, D. K. Murdoch, A. Antipenkov et al., "ITER fuel cycle R&D: Consequences for the design," *Fusion Engineering and Design*, vol. 81, pp. 733–744, 2006.

[10] Z. Zhu, B. Nie, and D. Chen, "A system dynamics model for tritium cycle of pulsed fusion reactor," *Fusion Engineering and Design*, vol. 118, pp. 5–10, 2017.

[11] F. Wang, R. Li, C. Ding et al., "Recent progress on the hydrogen storage properties of ZrCo-based alloys applied in International Thermonuclear Experimental Reactor (ITER)," *Progress in Natural Science: Materials International*, vol. 27, no. 1, pp. 58–65, 2017.

[12] R.-D. Penzhorn, M. devillers, and M. Sirch, "Evaluation of ZrCo and other getters for tritium handling and storage," *Journal of Nuclear Materials*, vol. 170, no. 3, pp. 217–231, 1990.

[13] R. A. Jat, S. C. Parida, J. Nuwad, R. Agarwal, and S. G. Kulkarni, "Hydrogen sorption-desorption studies on ZrCo-hydrogen system," *Journal of Thermal Analysis and Calorimetry*, vol. 112, no. 1, pp. 37–43, 2013.

[14] M. Devillers, M. Sirch, S. Bredendiek-Kämper, and R.-D. Penzhorn, "Characterization of the ZrCo-hydrogen system in view of its use for tritium storage," *Chemistry of Materials*, vol. 2, no. 3, pp. 255–262, 1990.

[15] S. Konishi, T. Nagasaki, and K. Okuno, "Reversible disproportionation of ZrCo under high temperature and hydrogen pressure," *Journal of Nuclear Materials*, vol. 223, no. 3, pp. 294–299, 1995.

[16] N. Bekris, U. Besserer, M. Sirch, and R.-D. Penzhorn, "On the thermal stability of the zirconium/cobalt-hydrogen system," *Fusion Engineering and Design*, vol. 49-50, pp. 781–789, 2000.

[17] M. Shim, H. Chung, S. Cho, and H. Yoshid, "Disproportionation characteristics of a zirconium-cobalt hydride bed under iter operating conditions," *Fusion Science and Technology*, vol. 53, no. 3, pp. 830–840, 2008.

[18] M. Hara, R. Hayakawa, Y. Kaneko, and K. Watanabe, "Hydrogen-induced disproportionation of Zr2M (M = Fe, Co, Ni) and reproportionation," *Journal of Alloys and Compounds*, vol. 352, no. 1-2, pp. 218–225, 2003.

[19] M. Devillers, M. Sirch, and R.-D. Penzhorn, "Hydrogen-induced disproportionation of the intermetallic compound ZrCo," *Chemistry of Materials*, vol. 4, no. 3, pp. 631–639, 1992.

[20] M. Hara, T. Okabe, K. Mori, and K. Watanabe, "Kinetics and mechanism of hydrogen-induced disproportionation of ZrCo," *Fusion Engineering and Design*, vol. 49-50, pp. 831–838, 2000.

[21] N. Bekris and M. Sirch, "On the mechanism of the disproportionate of ZrCo hydrides," *Fusion Science and Technology*, vol. 62, no. 1, pp. 50–55, 2012.

[22] R. A. Jat, R. Singh, S. C. Parida et al., "Structural and hydrogen isotope storage properties of Zr-Co-Fe alloy," *International Journal of Hydrogen Energy*, vol. 40, no. 15, pp. 5135–5143, 2015.

[23] R. A. Jat, S. C. Parida, R. Agarwal, and S. G. Kulkarni, "Effect of Ni content on the hydrogen storage behavior of ZrCo 1-xNix alloys," *International Journal of Hydrogen Energy*, vol. 38, no. 3, pp. 1490–1500, 2013.

[24] J. Wan, R. Li, F. Wang, C. Ding, R. Yu, and Y. Wu, "Effect of Ni substitution on hydrogen storage properties of Zr0.8Ti0.2Co1-xNix (x = 0, 0.1, 0.2, 0.3) alloys," *International Journal of Hydrogen Energy*, vol. 41, no. 18, pp. 7408–7418, 2016.

[25] Z. Huang, X. Liu, L. Jiang, and S. Wang, "Hydrogen storage properties of Zr1-xTixCo intermetallic compound," *Rare Metals*, vol. 25, no. 6, pp. 200–203, 2006.

[26] Y. Zhao, R. Li, R. Tang et al., "Effect of Ti substitution on hydrogen storage properties of Zr 1-xTixCo (x = 0, 0.1, 0.2, 0.3) alloys," *Journal of Energy Chemistry*, vol. 23, no. 1, pp. 9–14, 2014.

[27] R. A. Jat, S. Pati, S. C. Parida, R. Agarwal, and S. K. Mukerjee, "Synthesis, characterization and hydrogen isotope storage properties of Zr–Ti–Co ternary alloys," *International Journal of Hydrogen Energy*, vol. 42, no. 4, pp. 2248–2256, 2017.

[28] G. Zhang, G. Sang, R. Xiong, H. Kou, K. Liu, and W. Luo, "Effects and mechanism of Ti, Ni, Sc, Fe substitution on the thermal stability of zirconium cobalt-hydrogen system," *International Journal of Hydrogen Energy*, vol. 40, no. 20, pp. 6582–6593, 2015.

[29] H. Kou, G. Sang, W. Luo et al., "Comparative study of full-scale thin double-layered annulus beds loaded with ZrCo, Zr0.8Hf0.2Co and Zr0.8Ti0.2Co for recovery and delivery of hydrogen isotopes," *International Journal of Hydrogen Energy*, vol. 40, no. 34, pp. 10923–10933, 2015.

[30] R. A. Jat, R. Singh, S. Pati et al., "An analogy of interstitial site occupancy and hydrogen induced disproportionation of Zr1−xTixCo ternary alloys," *International Journal of Hydrogen Energy*, vol. 42, no. 12, pp. 8089–8097, 2017.

[31] W. T. Shmayda, A. G. Heics, and N. P. Kherani, "Comparison of uranium and zirconium cobalt for tritium storage," *Journal of the Less-Common Metals*, vol. 162, no. 1, pp. 117–127, 1990.

[32] H. Yoo, W. Kim, and H. Ju, "A numerical comparison of hydrogen absorption behaviors of uranium and zirconium cobalt-based metal hydride beds," *Solid State Ionics*, vol. 262, pp. 241–247, 2014.

[33] R. Sen, S. Das, and K. Das, "Microstructural characterization of nanosized ceria powders by X-ray diffraction analysis," *Metallurgical and Materials Transactions A: Physical Metallurgy and Materials Science*, vol. 42, no. 5, pp. 1409–1417, 2011.

[34] B. Joseph and B. Schiavo, "Effects of ball-milling on the hydrogen sorption properties of LaNi5," *Journal of Alloys and Compounds*, vol. 480, no. 2, pp. 912–916, 2009.

[35] A. Calka and D. Wexler, "Mechanical milling assisted by electrical discharge," *Nature*, vol. 419, no. 6903, pp. 147–151, 2002.

[36] M. H. Enayati, G. R. Aryanpour, and A. Ebnonnasir, "Production of nanostructured WC-Co powder by ball milling," *International Journal of Refractory Metals and Hard Materials*, vol. 27, no. 1, pp. 159–163, 2009.

[37] V. Batz, I. Jacob, M. H. Mintz, Z. Gavra, and J. Bloch, "The hydriding kinetics of massive ZrCo," *Journal of Alloys and Compounds*, vol. 325, no. 1-2, pp. 137–144, 2001.

[38] J. Bloch and M. H. Mintz, "Kinetics and mechanisms of metal hydrides formation - A review," *Journal of Alloys and Compounds*, vol. 253-254, pp. 529–541, 1997.

[39] H. Kou, W. Luo, Z. Huang et al., "Effects of temperature and hydrogen pressure on the activation behavior of ZrCo," *International Journal of Hydrogen Energy*, vol. 41, no. 25, pp. 10811–10818, 2016.

[40] M. Senna, P. Billik, A. Y. Yermakov et al., "Synthesis and magnetic properties of CuAlO2 from high-energy ball-milled Cu2O[sbnd]Al2O3 mixture," *Journal of Alloys and Compounds*, vol. 695, pp. 2314–2323, 2017.

[41] Y. Qi, X. Ju, C. Wan et al., "EXAFS and SAXS studies of ZrCo alloy doped with Hf, Sc and Ti atoms," *International Journal of Hydrogen Energy*, vol. 35, no. 7, pp. 2931–2935, 2010.

[42] M. Aureli, C. C. Doumanidis, I. E. Gunduz et al., "Mechanics and energetics modeling of ball-milled metal foil and particle structures," *Acta Materialia*, vol. 123, pp. 305–316, 2017.

[43] S. Rousselot, D. Guay, and L. Roué, "Comparative study on the structure and electrochemical hydriding properties of MgTi, Mg0.5Ni0.5Ti and MgTi0.5Ni 0.5 alloys prepared by high energy ball milling," *Journal of Power Sources*, vol. 196, no. 3, pp. 1561–1568, 2011.

[44] D. Lee, I. Kwon, J.-L. Bobet, and M. Y. Song, "Effects on the H2-sorption properties of Mg of Co (with various sizes) and CoO addition by reactive grinding," *Journal of Alloys and Compounds*, vol. 366, no. 1-2, pp. 279–288, 2004.

[45] J. Ženíšek, E. Kozeschnik, J. Svoboda, and F. D. Fischer, "Modelling the role of compositional fluctuations in nucleation kinetics," *Acta Materialia*, vol. 91, pp. 365–376, 2015.

[46] H. Zhang, R. Su, D. Chen, and L. Shi, "Thermal desorption behaviors of helium in Zr-Co films prepared by sputtering deposition method," *Vacuum*, vol. 130, pp. 174–178, 2016.

[47] S.-I. Orimo and H. Fujii, "Effects of nanometer-scale structure on hydriding properties of Mg-Ni alloys: A review," *Intermetallics*, vol. 6, no. 3, pp. 185–192, 1998.

[48] Y. Zhang, W.-S. Zhang, M.-Q. Fan et al., "Enhanced hydrogen storage performance of LiBH4-SiO 2-TiF3 composite," *The Journal of Physical Chemistry C*, vol. 112, no. 10, pp. 4005–4010, 2008.

[49] Q. Li, L.-J. Jiang, K.-C. Chou et al., "Effect of hydrogen pressure on hydriding kinetics in the Mg 2-xAgxNi-H (x = 0.05, 0.1) system," *Journal of Alloys and Compounds*, vol. 399, no. 1-2, pp. 101–105, 2005.

[50] H. Emami, K. Edalati, J. Matsuda, E. Akiba, and Z. Horita, "Hydrogen storage performance of TiFe after processing by ball milling," *Acta Materialia*, vol. 88, pp. 190–195, 2015.

[51] K. Edalati, J. Matsuda, M. Arita, T. Daio, E. Akiba, and Z. Horita, "Mechanism of activation of TiFe intermetallics for hydrogen storage by severe plastic deformation using high-pressure torsion," *Applied Physics Letters*, vol. 103, no. 14, Article ID 143902, 2013.

[52] K. Edalati, M. Matsuo, H. Emami et al., "Impact of severe plastic deformation on microstructure and hydrogen storage of titanium-iron-manganese intermetallics," *Scripta Materialia*, vol. 124, pp. 108–111, 2016.